Ophiolite Around the Indian Plate Margin

2

Ophiolite and ophiolitic rocks were emplaced along the western, northern and eastern margins of the Indian plate during the northward movement of the Indian plate and the collision of the Indian continental block first with intra-oceanic island arcs within the Neotethys, and then with the Helmand and Kabul continental blocks to the west (Tapponnier et al. 1981), the Asian continental block to the north (Gansser 1964) and the Myanmar continental block to the east (Mitchell 1993) (Fig. 1.2).

2.1 The Western Margin of the Indian Plate

The ophiolite belt along the western margin comprises the Bela, Muslim Bagh, Zhob and Waziristan-Khost ophiolites in Pakistan and bordering Afghanistan (Alleman 1979; Gnos et al. 1997) (Fig. 1.2). These and the related ophiolite belt along the southeastern coast of Oman were emplaced around the Cretaceous/Tertiary boundary. The western ophiolite belt of Pakistan consists of pyroxenite, gabbro and sheeted dikes deformed and metamorphosed at granulite to greenschist facies conditions. They are underlain by an accretionary wedge mélange containing slabs of pillow basalt intruded by microgabbro and associated with Early to Middle Cretaceous pelagic sediments. The mélange grades into calcareous turbidites of the Indian continental shelf.

2.1.1 Bela

The Bela Ophiolite is a dismembered sequence that presumably once formed a single thrust sheet. It consists of serpentinised mantle harzburgite overlain by layered peridotite and gabbro, foliated and isotropic gabbro, sheeted dikes and extrusive rocks (Gnos et al. 1998). The mantle rocks are underlain by a poorly preserved metamorphic sole of amphibolite to greenschist facies rocks. Foliated and undeformed granitoid plutons are common within the crustal section that yielded $^{40}Ar/^{39}Ar$ plateau ages of 69.5 ± 0.7 Ma and 68.7 ± 0.7 Ma from amphibole separates (Gnos et al. 1998). The granitoid plutons comprise gabbro, diorite, trondhjemite, plagiogranite and granite. Chemical composition of the plagiogranite is consistent with its origin from fractional crystallisation of basaltic magma, and U–Pb zircon dating of trondhjemite and granite yielded an age of 68 ± 3 Ma (Ahmed 1993). These ages constrain the age of origin and emplacement of the ophiolite. The accretionary wedge unit below the ophiolitic unit contains imbricate sheet of pillow basalt with E-MORB-type chemistry covered by radiolarian chert, shale and calciturbidites and capped by Reunion hotspot-related lavas.

2.1.2 Muslim Bagh and Waziristan

The Muslim Bagh ophiolite is related to a WSW-ENE trending thrust, and occurs in the uppermost part of a pile of nappes accreted onto the Indian continental margin (Asrafullah et al. 1979; Ahmad and Abbas 1979). The ^{40}Ar-^{39}Ar plateau age of the Muslim Bagh ophiolite is 70.7 ± 5.0 Ma for the metamorphics, and 68.7 ± 1.8 Ma for the amphibolites at the base of the sheeted dykes (Mahmood et al. 1995). It seems that the floor of the Neotethys Sea was subducted 65–70 many years ago in the Pakistan sector (Valdiya 2010).

The Paleocene-Early Eocene Waziristan ophiolite (~ 500 km^2) is the third largest ophiolite complex in Pakistan after Bela and Zhob (Jan et al. 1985). It occurs as dismembered thrust slices tectonically overriding Jurassic-Cretaceous calcareous sediments of the Indian plate. It consists of ultramafics rocks, gabbro, sheeted dikes, pillow lava, plagiogranite, anorthosite and pelagic sediments. The sedimentary rocks associated with the ophiolite are Mesozoic and Early Tertiary in age. The ultramafics include harzburgite, dunite, pyroxenite and secondary serpentinite, and display deformational features and cataclastic fabrics similar to those in the Zhob and Jijal complexes. The sheeted dikes show chilled margins. Some trondhjemite

N. C. Ghose et al., *A Petrographic Atlas of Ophiolite*,
DOI: 10.1007/978-81-322-1569-1_2, © Springer India 2014

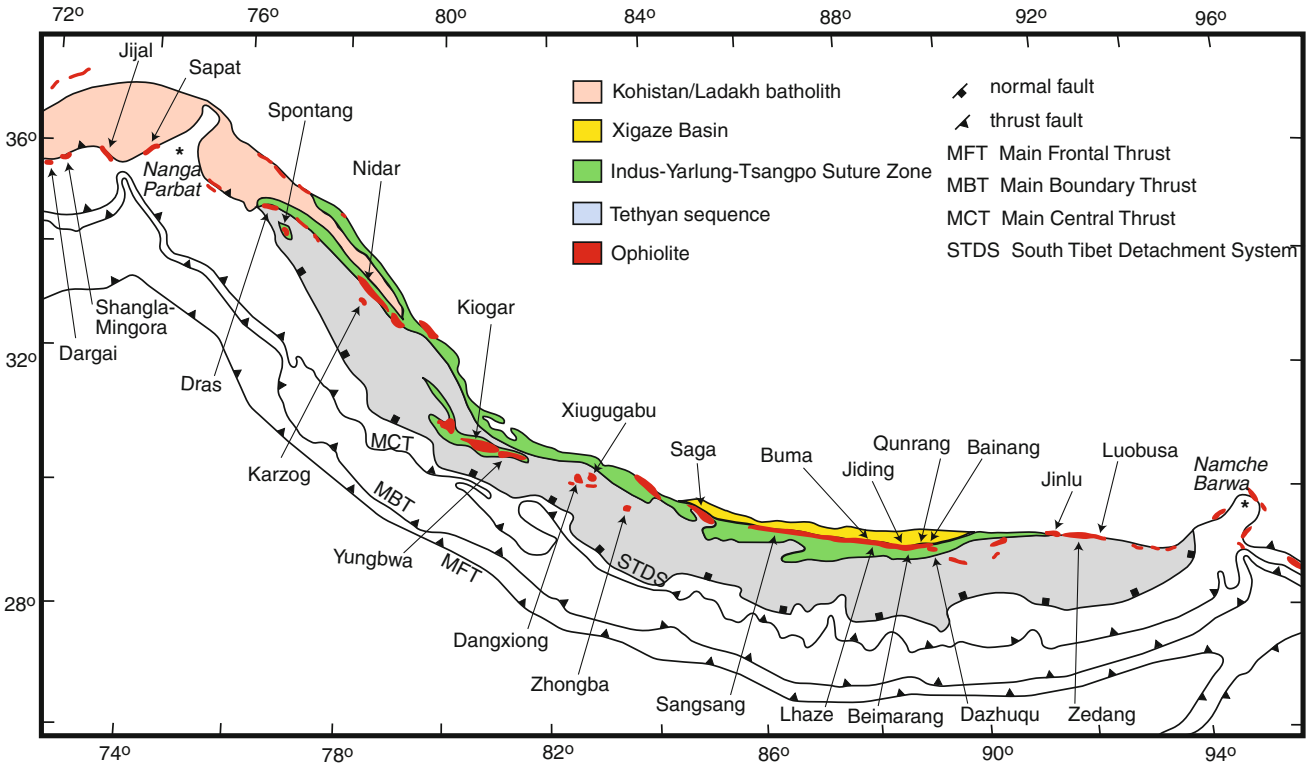

Fig. 2.1 Himalayan ophiolite complexes (after Hébart et al. 2012)

dikes containing sodic plagioclase show a calc-alkaline affinity. The volcanic rocks commonly showing pillow structures comprise about half of the total area of the ophiolite complex. Subordinate occurrence of agglomerate and volcanic tuffs are noteworthy features.

2.2 The Northern Margin of the Indian Plate

According to our present understanding, ophiolitic rocks at the northern margin of the Indian plate originated between Jurassic and Early Cretaceous in mid-oceanic ridges and supra-subduction zones of intra-oceanic arc systems within the Neotethys Ocean (Aitchison et al. 2003; Aitchison and Davis 2004). Geochemical data indicate that the ophiolitic rocks formed in fore-arc, arc and back-arc setting from mixed magmas including calc-alkaline, mid-oceanic ridge basaltic and oceanic-island basaltic magmas (Hébart et al. 2012). These rocks were obducted southwards onto the Indian plate margin or accreted within the Indus-Yarlung-Tsangpo Suture Zone (Thakur 1981) as the Indian continental block collided with the intra-oceanic arc in Late Cretaceous and with the Asian continent in Paleocene-Eocene as the Neotethys closed (Tapponnier et al. 1981; Allègre et al. 1984; White and Lister 2012). The Indus-Yarlung-Tsangpo Suture continues into the Central Myanmar Basin in the east and to Baluchistan in the west (Valdiya 1988, 2010). A variety of assemblages of sediments that were deposited in the northwestern part of the suture zone are known as the Indus Flysch. Some of the ophiolites along the suture zone were emplaced as thrust sheets on the Indian continental margin and presently occur as klippen on deep-water marine sedimentary sequences of the Indian passive margin, whereas others occur as well-preserved or dismembered sections and mélanges within the Indus-Yarlung-Tsangpo Suture Zone (Gansser 1964, 1980).

2.2.1 The Indus Suture Zone

The ophiolite occurrences along the Indus Suture Zone include the Dargai, Shangla-Mingora, Jijal and Sapat complexes on the western side of the Nanga Parbat syntaxis in northern Pakistan (reviewed in Arif and Jan 2006) and the Dras, Spontang and Nidar-Karzog complexes on the eastern side of the syntaxis in eastern Jammu and Kashmir, India (reviewed in Mahéo et al. 2004) (Fig. 2.1).

2.2.1.1 Sapat

The Sapat and Jijal complexes are located on the hanging wall of the north-dipping Indus Suture Zone and constitute the southernmost part of the Kohistan Arc (Fig. 2.1).The Sapat Complex consists of two lithological units. The lower

unit comprises ultramafic rocks such as meta-harzburgite, dunite and intrusive clinopyroxenite (Bouilhol et al. 2009). Meta-harzburgite displays a massive, fine-grained texture with relict orthopyroxene and disseminated spinel grains. The olivine porpyroblasts are lobate in shape with sub-grain boundaries. They show undulose extinction and are surrounded by fine-grained, undeformed olivine neoblasts. Small euhedral spinel grains are present within the olivine pophyroblasts, and amoeboid spinel grains are associated with the olivine neoblasts. The matrix also contains orthopyroxene decomposition products such as olivine, talc and tremolite that indicate fluid-assisted lower amphibolite facies re-equilibration. Secondary chlorite around spinel, serpentine and rare diopside around olivine and calcite vein in dunite have been observed. The dunites are fresh and coarser and contain trails/pods of chromite spinel and clinopyroxene that may have originated through melt percolation. Olivine-clinopyroxene micro-veins and thin dikes are interpreted as melt crystallisation products. Mineral and bulk rock compositions and U-shaped REE patterns suggest that the meta-harzburgites represent a refractory, metasomatised mantle.

The ultramafic unit is bounded by a fault zone at the top and is overlain by meta-gabbro and tonalite–trondhjemite with clinopyroxenite intrusives. The olivine-bearing clinopyroxenites occur as sub-horizontal bands below metaplutonic rocks, vertical intrusive bodies with gabbro and tonalite-trondhjemite cores, and dikes. Clinopyroxene overgrows olivine in the clinopyroxenites. Amoeboid clinopyroxene occurs at the grain boundaries of olivine porphyroblasts. Trails of lobate clinopyroxene porphyroblasts are also present. Secondary chlorite and hornblende are associated with clinopyroxene. Geochemical modelling indicates that the parental melt of the pyroxenites and metagabbros was a highly depleted primitive arc melt of suprasubduction affinity (Bouilhol et al. 2009).

2.2.1.2 Dras

In the Ladakh-Zanskar area of the northwestern Himalayas, the NW–SE Indus Suture Zone separates the Ladakh Batholith of the Asian margin to the NE from the Zanskar and Tethys Himalayas of the Indian margin to the SW (Fig. 2.1). The NW part of the Indus Suture Zone comprises a northern unit known as the Indus Group with continental molasse-type sediments, and an ophiolite-bearing southern unit containing the Dras Arc. The Dras Complex is composed of island arc calc-alkaline and tholeiitic basalts intruded by granodioritic plutons (Dietrich et al. 1983; Radhakrishna et al. 1984). The arc-related units are stratigraphically underlain by blocks of ophiolitic rocks such as serpentinised harzburgite, lherzolite tectonite, cumulate dunite, pyroxenite and intrusive gabbro and diabase (Srikantia and Razdan 1980 , 1985; Srikantia 1986; Radhakrishna et al. 1987; Reuber et al. 1989). The Dras Ophiolite is marked by a basal fault and is underlain by the Sapi-Shergol ophiolitic mélange containing 90 Ma blueshists (Honegger et al. 1989). The mélange, the ophiolite and the Dras Arc units are tectonically overlain by the Lamayuru Formation and the Zanskar shelf succession of the Indian margin along a south-dipping back-thrust (Sinha and Upadhyay 1993; Robertson and Degnan 1993).

U–Pb zircon ages of 103 ± 3 Ma (Honegger et al. 1982) and 101 ± 2 Ma (Schärer et al. 1984) of granodiorite intrusives in the Dras volcanic and volcaniclastic rocks constrain the minimum age of the Dras Ophiolite. K–Ar ages of 77.5 ± 1 Ma (Sharma et al. 1979) and 78.5 ± 2.9 Ma (amphibole separate, Reuber et al. 1989) indicate Late Cretaceous metamorphism of the Dras Complex.

2.2.1.3 Spontang

About 75 km SE of Dras and south of the Indus Suture, the Spontang Ophiolite occurs in a tectonic thrust slice above the Paleocene-Eocene carbonate sequence of the Zanskar Himalaya (Fig. 2.1). The ophiolite sequence consists of weakly foliated mantle harzburgite and spinel-lherzolite intruded by diorite and rare plagiogranite, cumulates of gabbro and ultramafic rocks, isotropic gabbro, highly tectonised sheeted dikes with intrusive plagiogranite feeding pillow lava of N-MORB-type geochemical signature (Corfield et al. 2001). The mantle units may be divided into a lower and an upper section separated by a south-dipping thrust. The lower section consists of serpentinised peridotites (up to 98 % serpentine near the top), whereas the upper section consists of fresh peridotites (Mahéo et al. 2004). Both sections are cross-cut by dunitic and dioritic dikes and sills. The mantle rocks are composed of porphyroclastic olivine and pyroxenes. Orthopyroxene commonly shows lobate boundaries interpreted as evidence of mantle melting. Temperatures of 1000–1200 °C at low deviatoric stress have been inferred from kinked olivine in peridotite that originated through high-temperature plastic flow during ascent of the upper mantle and partial melting below a spreading centre (Reuber 1986). Plagioclase laths in the upper crustal gabbro are well preserved but commonly altered, indicating that they crystallised before clinopyroxene in a normal mid-oceanic ridge environment (Corfield et al. 2001). The diorites dikes and sills cross-cutting the mantle peridotites have ophitic to cumulate textures. They are dominated by metamorphic amphibole and albitic plagioclase with minor amounts of oxides, apatite, epidote and titanite (Mahéo et al. 2004). Magmatic relics occur in the plagioclase cores and as diopsidic clinopyroxene inclusions in hornbende and edenitic amphibole. Hornblende is locally replaced by actinolite or ferro-actinolite. The ophiolite sequence is unconformably overlain by basalt, andesite and volcano-sedimentary rocks of the Spong arc that developed over the fore-arc of the supra-subduction zone. The

Spontang ophiolitic mélange containing Permo-Triassic and Albian alkaline magmatic rocks tectonically underlies the ophiolite sequence. Structural, tectonic and palaeomagnetic constraints indicate that the Spong Arc and the Dras Arc were separate but coexisting intra-oceanic island arcs (Corfield et al. 2001).

U–Pb zircon dating of N-MORB-type plagiogranite intrusive in sheeted basaltic dike indicates that the oceanic crust of the Spontang Ophiolite formed at 177 ± 1 Ma in a mid-oceanic ridge environment, making it one of the oldest of the Tethyan ophiolites discovered so far (Pedersen et al. 2001). Moreover, incompatible trace element data including REE and $^{39}Ar/^{40}Ar$ dating of amphiboles in intrusive diorite in peridotite indicate that the mantle source of the N-MORB-type basalts was metasomatised in a supra-subduction zone at c. 130 Ma during the initiation of subduction (Mahéo et al. 2004). Recent fossil evidence suggests that intra-oceanic subduction may have continued until c. 55 Ma (Baxter et al. 2010). An 88 ± 5 Ma date from andesite in the Spong arc indicates that the arc was still active at c. 88 Ma and obduction of the ophiolite on the Indian continental margin occurred after c. 88 Ma (Pedersen et al. 2001). Based on field evidence, Corfield et al. (2005) suggest that thrusting of the ophiolite over the Cenozoic Zanskar sediments was a younger event that happened during the India-Asia collision in late Paleocene-early Eocene. However, Garzanti et al. (2005) disagree with the field evidence of Corfield et al. (2005) and contend that the ophiolite was obducted on the Indian margin in Early Eocene.

2.2.1.4 Nidar and Karzog

Further east, the Nidar Ophiolite delineates the southern margin of the Indus Suture Zone in eastern Ladakh (Fig. 2.1). It has a south-dipping thrust contact with the Indus Formation in the north, and a north-dipping thrust contact with the blueschist-bearing Zildat ophioliticmélange (Virdi et al. 1977; Virdi 1987, 1989; Thakur and Misra 1984). Both the ophiolite and the Zildat mélange are thrust over the Tso-Morari crystalline complex in the south. Petrological and geochemical data including isotopes indicate that the ophiolite originated in an intra-oceanic subduction environment (Ahmad et al. 2008). The ophiolite is composed of ultramafic rocks at the base, gabbroic rocks in the middle and volcano-sedimentary rocks at the top. The ultramafics include spinel–harzburgite near the base, spinel–dunite with chromite veins at higher levels and minor pyroxenite intrusives that also occur in the overlying gabbros. Both microgabbro with ophitic texture and cumulate gabbros are present. The gabbros consist of olivine, clinopyroxene, plagioclase and amphibole with minor interstitial magnetite and spinel (Ahmad et al. 2008). Olivine occurs as large lobate grains, smaller euhedral grains at margins of porphyroclasts and as inclusion within plagioclase and clinopyroxene. Clinopyroxene occurs as oikocrysts with olivine and plagioclase inclusions, and smaller interstitial grains. Some large plagioclase grains show kink bands and bent cleavage overgrown by undeformed rims. The cores of the large clinopyroxene have lower calcium contents than the undeformed rims. Amphibole occurs as rims around clinopyroxene or in late-stage veins. Many gabbro samples consist of metamorphic assemblage of hornblende + albitic plagioclase (Mahéo et al. 2004). The pargasitic amphiboles range in composition from magnesio-hornblende to actinolite characteristic of oceanic metamorphism. Anorthite-rich cores of plagioclase low-Ti diopside inclusions in hornblende are interpreted as magmatic relics. Plagiogranite intrusives within the gabbro showing nearly flat REE patterns originated through fractional crystallisation of subalkalinetholeiitic magmas (Rao et al. 2004).

The volcano-sedimentary unit contains porphyritic basalt and andesite with poorly preserved pillow structures near its base, and gradually passes into volcaniclastics comprising chert, jasper, shale, siltstone, volcanic sandstones and conglomerates. The upper part of the volcano-sedimentary unit is dominated by andesite and rhyolite intercalated with ash, tuff, lapilli and volcanic breccia. The phenocryst in basalts show evidence of hydrothermal alteration and is dominated by albitic plagioclase laths, diopside-augite and serpentinised olivine, and minor Fe–Ti oxides. The groundmass is composed of fine-grained augite, plagioclase and rare glass. Epidote and radiating crystals of chlorite are also present in the groundmass. The rhyolites show banding and are dominated by volcanic glass and feldspar spherules with minor mafic phases such as pyroxene and fibrous chlorite. Palagonite is commonly associated with the glass. Calcite and quartz veins and vesicles with quartz filling are observed in some samples.

The Tso-Morari crystalline complex, an exhumed block of the subducted Indian continental crust containing eclogite, is located to the immediate south of the Nidar Ophiolite (Berthelsen 1953). A small section of ophiolite consisting of highly deformed and altered chromitite, serpentinite and minor gabbro occurs at the southern margin of the Tso-Morari dome near Karzog. The Karzog ophiolite is presumably a detached klippe of the Nidar Ophiolite (de Sigoyer et al. 2004). The mafic rocks comprise large poikilitic metamorphic edenitic amphibole with relics of low-Ti diopside, albite, oxides and greenschist facies minerals such as actinolite, titanite and epidote (Mahéo et al. 2004).

Gabbro and basalt from the Nidar Ophiolite yielded an Sm–Nd isochron age of 140 ± 32 Ma that indicates the time of formation of the ophiolitic crust (Ahmad et al. 2008). Amphiboles in the Nidar gabbro yielded ages between 100 and 120 Ma by $^{39}Ar/^{40}Ar$ step-heating technique that

probably corresponds with metamorphism related to the initiation of subduction (Mahéo et al. 2004). Radiolarian taxonomy and biostratigraphy reveal an upper Barremian to Upper Aptian age for the Nidar volcano-sedimentary section (Zyabrev et al. 2008), consistent with the $^{39}Ar/^{40}Ar$ amphibole age of Nidar gabbro.

2.2.2 The Yarlung-Tsangpo (Yarlung-Zangbo) Suture Zone

2.2.2.1 The Western Part

The ophiolites in the western part of the Yarlung-Tsangpo Suture Zone occur along the suture zone itself as well as to the south of suture zone as klippen overlying an ophiolitic tectonic mélange (Hodges 2000; Searle et al. 1988). The klippe-type ophiolites include the Kiogar, Yungbwa, Dangxiong, Xiugugabu and Zhongba massifs (Fig. 2.1). Recent U–Pb zircon dating on diabase and tholeiite yielded ages of 123.4 ± 0.9 Ma and 123.9 ± 0.9 Ma for the Yungbwa and 126.7 ± 0.4 Ma and 123.4 ± 0.8 Ma for the Dangxiong (Chan et al. 2007), 120.2 ± 2.3 Ma for the Yungbwa (Li et al. 2008) and 122.3 ± 2.4 Ma for the Xiugugabu (Wei et al. 2006) and 125.7 ± 0.9 Ma for the Zhongba (Dai et al. 2012) massifs. These dates are younger than the 159.7 ± 0.5 Ma U–Pb zircon age of the Kiogar gabbro (Chan et al. 2007), and the earlier determined 152 ± 33 Maage of hornblende in the Yungbwa massif by the $^{40}Ar/^{39}Ar$ isotope method (Miller et al. 2003). The tectonic mélange underlying the ophiolites contains clasts of Late Jurassic to Early Cretaceous radiolarite (Dai et al. 2011) and older rocks including reef and micritic limestone and mafic rocks. The mélange overlies rocks of the Indian continental passive margin.

The Yungbwa Ophiolite is a large peridotitic complex tectonically overlying a mélange that contains blocks of Permian reef limestone, Late Cretaceous micritic limestone and volcanic rocks. It is located in SW Tibet, about 20 km south of the Indus-Yarlung-Tsangpo Suture Zone, south of Mount Kailas, and to the immediate NW of the Gurla Mandhata crystalline complex. The ophiolite and the mélange are thrust over sediments of the Tethyan series to the south. The main constituent of the ophiolite is clinopyroxene-bearing, serpentinised spinel-harzburgite that is cross-cut by dikes of basalt, gabbro and gabbronorite (Miller et al. 2003; Liu et al. 2010). Similar rocks occur in the Kiogar Ophiolite located to the immediate NW of the Yungbwa massif (Gansser 1964). Fresh harzburgite from the Yungbwa massif shows porphyroclastic texture and contains elongated olivine with kink-bands and orthopyroxene with exsolution lamellae and deformed cleavage showing undulatory extinction, and arranged sub-parallel to the foliation. Large spinel grains have "holly-leaf" shape. Orthopyroxene compositions are within the range of orthopyroxenes in abyssal peridotites, and temperatures based on two-pyroxene equilibria are 900–960 °C and on olivine-spinel Mg–Fe exchange are 760 °C (Miller et al. 2003). The lower temperature is similar to temperatures calculated in peridotite tectonite from slow spreading ridges (Constantin 1999). Pyroxene inclusions have been observed in plagioclase. The interstitial grains comprise neoblasts of olivine, orthopyroxene and clinopyroxene with well-defined crystal shapes, rounded spinel and disseminated sulphides. Mineral chemistry and Os-isotopic ratio of the peridotites are similar to those of abyssal peridotites, and Nd model age of clinopyroxene indicates that the peridotites underwent melt extraction in Jurassic (Miller et al. 2003). Minor plagioclase and amphibole are unevenly distributed in the harzburgites (Liu et al. 2010). Amphibole also occurs as blebs within orthopyroxene, and as interstitial grains aligned with the clinopyroxene exolution lamellae. Anhedral plagioclase commonly replaces clinopyroxene and orthopyroxene. The pargasitic amphibole and anorthitic plagioclase originated through metasomatic alteration of the mantle with a high-Ca, high-LREE and low-Ti arc-type hydrous melt in a subduction zone setting (Liu et al. 2010).The bulk REE and Nd-isotopic compositions of peridotite also indicate secondary syn- or post-emplacement modification of the ophiolite (Miller et al. 2003). The basaltic dikes show subophitic orhypidiomorphic-granular texture and consist of diopsidic augite, plagioclase, minor hornblende and accessory ilmenite. They are tholeiitic and show N-MORB-type REE patterns. Sericitisation of plagioclase and replacement of clinopyroxene and hornblende byactinolite indicate low-grade metamorphism. The gabbronorite dikes show sharp contacts with the host peridotites and consist of clinopyroxene, orthopyroxene and plagioclase with 120° triple junctions. Their primary textures are modified by recrystallisation and granulation. Plagioclase shows undulatory extinction and is partially transformed into prehnite-bearing saussurite. Clinopyroxene is partially replaced by metamorphic hornblende, tremolite or actinolite with a typical flaser texture.

The Xiugugabu massif is dominated by variably serpentinised harzburgite intruded by amphibole-bearing microgabbro and microgabbronoritesills sub-parallel to foliation, and isolated outcrops of red and green chert. Geochemical characteristics of the harzburgites indicate that they are residues of 5–25 % of partial melting of a depleted mantle that has been enriched by percolating metasomatic melts in a supra-subduction environment (Bezard et al. 2011). Dunite is rare and occurs in patches within harzburgite. The harzburgites display porphyroclastic to porphyromylonitic texture and consist of kinked and highly stretched olivine and orthopyroxene porphyroclasts showing undulatory extinction. Orthopyroxene contains

clinopyroxene exsolution lamellae and are surrounded by neoblasts. Minor spinel occurs as large euhedral grains and small vermicular intergrowths. Accessory magnetite, chlorite and amphibole are present. The microgabbro and microgabbronorite sills comprise plagioclase and pyroxene microphenocrysts oriented along the foliation, and a groundmass of amphibole, plagioclase, clinopyroxene and orthopyroxene, ilmenite and magnetite with secondary epidote, chlorite and sericite. The textural relation indicates that plagioclase crystallised before pyroxene. The amphiboles likely originated in a high-T (~ 800 °C) hydrothermal environment. Metamorphic textures such as magnetite + clinopyroxene symplectite, amphibole + clinopyroxene symplectite and amphibole overgrowth around clinopyroxene have been observed. The intrusive rocks have tholeiitic compositions and show N-MORB-type REE pattern, Th enrichment and Nb, Ta and Ti negative anomalies, indicating a back-arc, supra-subductionzone setting.

The Zhongba massif consists of mantle ultramafics, and a crust composed of diabase dikes and pillow basalts (Dai et al. 2012). It is surrounded by a mélange containing blocks of massive basalt associated with layers of deformed limestone, black shale and purple-red and green-grey chert. The mantle ultramafics are dominated by fresh foliated harzburgite with minor dunite. A diabase dike shows granular to medium-grained intersertal texture with idiomorphic plagioclase, chloritised pyroxene and olivine and minor Fe–Ti oxides. Porphyritic pillow and massive basalts consist of phenocrysts of plagioclase, clinopyroxene and olivine in a fine-grained, intersertal to intergranular groundmass of plagioclase, clinopyroxene and Fe–Ti oxides, and secondary veins and amygdules of carbonate, quartz and chlorite. Some of the phenocrysts are partially or completely replaced by albite or chlorite. Texture showing clinopyroxene cores with radiating plagioclase laths is present in some samples. The mafic rocks exhibit an ocean-island and Hawaiian alkali basalt-type REE pattern that suggests an origin from a series of seamounts within the Neo-Tethys during the Early Cretaceous (Dai et al. 2012).

2.2.2.2 The Central Part

The central part of the Yarlung-Tsangpo Suture Zone contains a series of ophiolite massifs including the Saga and Sangsang ophiolites in the west and the Xigaze ophiolites (from west to east: Buma, Lhaze, Jiding, Beimarang, Qunrang, Bainang and Dazhuqu massifs) in the east (Fig. 2.1). U–Pb zircon dating in diorite, gabbro and diabase yielded ages of 125.2 ± 3.4 Ma for the Sangsang massif (Xia et al. 2008b), 128 ± 2 Ma for the Jiding massif Wang et al. 2006), 125.6 ± 0.8 Ma for the Bailang massif (Li et al. 2009) and 126 ± 1.5 Ma for the Dazhuka massif (Malpas et al. 2003). Plagiogranite from the Xigaze ophiolitic crust yielded an age of 120 ± 10 Ma (Göpel et al.1984), and apegmatitic gabbro yielded an age of 132.0 ± 2.9 Ma (Chan et al. 2007). Hornblende in amphibolite in the Buma and Bailang massifs yielded similar dates of 123.6 ± 2.9 Ma, 127.7 ± 2.2 Ma and 127.4 ± 2.3 Ma with the $^{40}Ar/^{39}Ar$ step-heating technique (Guilmetteet al. 2008, 2009). Radiolarites from above the volcanic rocks in the Bailang massif confirm these ages (Zyabrev et al. 1999, 2008).

The Saga and Sangsang ophiolites are located about 200–350 km west of Xigaze. They consist of mantle peridotites overlain by leuco- and melano-gabbros, and a mafic crust consisting of brecciated basalt, lava, diabase and amphibolite overlain by sandstone with chert. Field and geochemical data suggest that they formed in the arc or back-arc of an intra-oceanic supra-subduction zone(Bedard et al. 2009). In the south, the massifs are underlain by an ophioliticmélange containing blocks of strongly foliated garnet- and clinopyroxene-bearing amphibolite, serpentinite, diabase, gabbro and sedimentary rocks. The high-grade metamorphic rocks in the mélange, showing peak P–T conditions of 12 kb/850 °C, ages of 123–128 Ma and bulk composition similar to MORB, E-MORB and back-arc basalt indicate the presence of a metamorphic sole under the ophiolite massifs that formed contemporaneously with the ophiolitic crust (Guilmette et al. 2009, 2012). The blocks of gabbro show LREE depletion and are composed of magmatic plagioclase, diopside-augite clinopyroxene and brown amphiboles such as tschermakite and magnesiohorn blende and minor ilmenite and titanite (Dupuis et al. 2005). Further south, the ophiolitic mélange is underlain by the Yamdrock tectonic mélange comprising imbricate thrust sheets representing slices of the ocean floor including red siliceous shale, radiolarian chert and minor alkaline basalt. Mafic rocks from the Yamdrock mélange and from the underlying Triassic flysch of the Indian passive margin show LREE enrichment, and are similar to the volcanic rocks of the Reunion hotspot and the Deccan basalts of India (Dupuis et al. 2005).

The mantle lherzolites and harzburgites in the Saga massif are relatively fresh with secondary serpentine only in small veins or localised domains, whereas harzburgite in the Sangsang ophiolite is more affected by serpentinisation especially near faults or shear zones. The large olivine and pyroxene grains show minor folds or kinks and undulatory extinction. Olivine inclusions are present in pyroxene. Minor spinel occurs as euhedral grains. Recrystallised, interstitial fine-grained olivine around clinopyroxene, olivine + clinopyroxene symplectite around orthopyroxene, orthopyroxene + spinel symplectite and vermicular spinel have been interpreted as evidence of melt-rock interactions (Bedard et al. 2009 and references therein). Minor chlorite, actinolite, carbonate and prehnite occur as products of secondary alteration and metasomatism. The gabbros are composed of sub-idiomorphic plagioclase altered to

albite + prehnite, sub-idiomorphic to allotriomorphic clinopyroxene replaced by metamorphic green amphibole or minor chlorite, rare brown igneous amphibole and rare orthopyroxene. Minor titanite and prehnite veinlets are also present. The uppermost part of the mafic crust contains brecciated lava with clasts of pyroxene altered to actinolite and chlorite, plagioclase and quartz, set in a greenish-brown matrix of recrystallised plagioclase, minor chlorite, quartz, carbonate and prehnite in veins. Mafic to intermediate lavas contain altered clinopyroxene, plagioclase microlites and glomerocrysts (with pyroxene inclusions) altered to albite, prehnite and/or sericite and minor oxides. Amygdules filled with chlorite, quartz and carbonate and carbonate and chlorite veinlets are also observed in the lavas. Diabase contains fresh plagioclase, altered clinopyroxene, orthopyroxene and minor secondary actinolite needles and epidote. Amphibolite containing cloudy plagioclase, metamorphic green hornblende and minor oxides and titanite is highly altered to albite-prehnite-epidote-chlorite assemblages. Sandstone contains clasts of deformed quartz, feldspar, pseudomorphs of pyroxene and hornblende with actinolite and chlorite, spinel, felsic plutonics, mafic to intermediate volcanics, rare radiolarian chert and carbonate oolite and minor chlorite and carbonate.

In the Xigaze area, several dismembered ophiolite complexes occur along the Yarlung-Tsangpo Suture between the Xigaze fore-arc flysh in the north and the Mesozoic Yamdrock mélange and Triassic flysch of the Tethyan series in the south (Nicolas et al. 1981; Girardeau et al. 1985a, b; Girardeau and Mercier 1988). The mantle units consist of well foliated, variably serpentinised, spinel-bearing dunite and harzburgite at the top grading downward to Cr-diopside harzburgite and lherzolite that equilibrated at 1155–1255 °C and 5–11 kb indicating a slow-spreading ridge environment (Girardeau and Mercier 1988). Harzburgites in the western massifs contain porphyroclastic orthopyroxene with clinopyroxene exsolution lamellae that are surrounded by granoblastic olivine showing slip planes and kink bands. Their geochemical and isotopic characteristics indicate that they are residues of 7–12 % melting of an N-MORB-type mantle source in a back-arc setting (Dubois-Côté et al. 2005). On the other hand, peridotites in the eastern massifs consisting of granular orthopyroxene and olivine with interstitial Cr-diopside represent metasomatically altered residues of 30–40 % melting of a depleted mantle source in an intra-oceanic arc environment. Concordant to discordant orthopyroxene bands, websterite veins, and irregular and tabular dunite lenses are common in the peridotites. Rodingitised diabase and gabbro dikes commonly occur in the upper part of the mantle unit. The crustal rocks are primarily made of diabase sheeted dikes and sills, and extrusives. Lower crustal ultramafic–mafic rocks are minor, and volcaniclastic rocks are very rare. Pillow lava is altered and contains a few vesicles filled with quartz, calcite, chlorite and/orepidote. Microphenocrysts of plagioclase and clinopyroxene in basalts display intersertal texture. Rare hornblende phenocrysts are present in a diabase dike. Subordinate glass and opaques are present in the groundmass. Secondary actinolite and clay minerals are commonly observed.

2.2.2.3 The Eastern Part

The eastern part of the Yarlung-Tsangpo Suture Zone includes the Jinlu, Zedang and the Luobusa massifs (Fig. 2.1, 2.2a). The intrusives and volcanics of the Zedang massif have been dated at 161 ± 2.3 Ma by the U–Pb zircon method in dacite, and 152.2 ± 3.3 Ma by $^{40}Ar/^{39}Ar$ step heating of hornblende in andesitic dike (McDermid et al. 2002). U–Pb dating of zircon in diabase yielded ages of 149.7 ± 3.4 Ma, 150.0 ± 5.0 Ma (Chan et al. 2007) and 162.9 ± 2.8 Ma (Zhong et al. 2006) for the Luobusa massif.

The Luobusa Ophiolite is overthrust northward onto the Gangdese Batholith of the Asian margin (Lhasa Terrane) and onto the Tertiary molasse-type deposits of the Luobusa Formation (Zhou et al. 1996). A south-dipping thrust separates the ophiolite complex from a thick Triassic flysch sequence in the south. The mantle sequence consists of coarse-grained harzburgite and diopsidic harzburgite well-developed porphyroclastic texture. Chromite compositions indicate that the harzburgites are residua left after extraction of MORB-type magmas. Rare olivine porphyroclasts contain orthopyroxene inclusions and show deformation lamellae and kink bands. Olivine replaces orthopyroxene as indicated by fine-grained olivine neoblasts in the granoblastic matrix surrounding subhedral to anhedral orthopyroxene porphyroclasts with clinopyroxene lamellae. Accessory chromite is anhedral and ubiquitous. Dunites occur as lenses or as envelopes around podiform chromitites in the peridotites. The upper part of the peridotite sequence, described as a transition zone (Zhou et al. 1996), is sheared and primarily consists of dunite grading into wehrlite. Chromite occurs as euhedral inclusions in olivine in dunite as well as fine-disseminated grains in thin layers. A mélange zone tectonically overlies the transition zone and contains deformed cumulate lenses, pillow lava and mid-Cretaceous marine sedimentary rocks of the Zedong Formation in a serpentinised ultramaficmatrix.

2.2.2.4 The Namche Barwa Syntaxis

Sporadic lenses of metamorphosed mafic–ultramafic rocks of a dismembered mélange suite occur in the Yarlung-Tsangpo Suture Zone of this area (Quanru et al. 2006) (Figs. 2.1, 2.2a). These rocks include diabase and amphibolite of boninite, arc tholeiite and back-arcbasalt affinity indicating origin in a supra-subduction zone environment.

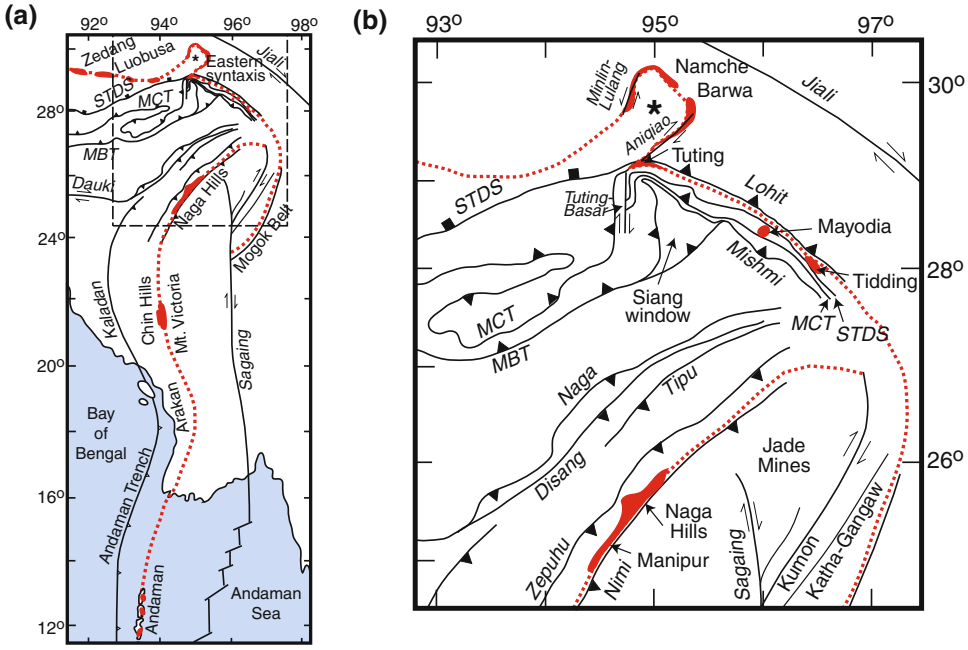

Fig. 2.2 Ophiolite complexes along the eastern margin of the Indian plate: **a** regional setting, **b** detailed view of the area demarcated by *dashed lines* in (**a**). The symbols are as in Figs. 2.1 and 2.2. The names of the faults are italicised. Compiled from Bhattacharjee 1991; Ding et al. 2001; Ghosh et al. 2007; Misra 2009; Mitchell 1993; Mitchell et al. 2007; Saha et al. 2012; Searle et al. 2007; Singh and Singh 2011; Quanru et al. 2006; Yin et al. 2010

2.3 The Eastern Margin of the Indian Plate

At the eastern Himalayan syntaxis, the collision of the Indian block with Asia is accommodated by a pair of roughly NE–SW strike-slip faults along the northwestern (Minlin-Lulang sinistral fault) and southeastern (Aniqiao dextral fault) boundaries of the Namche Barwa massif (Burg et al. 1998; Ding et al. 2001; Quanru et al. 2006). The Yarlung-Tsangpo suture follows these faults, swerves around Namche Barwa and its trend becomes southwestward (Fig. 2.2). Southwest of Namche Barwa, the Aniqiao fault is continuous with the N–S trending Tuting-Basar dextral strike-slip fault (Acharyya and Saha 2008; Saha et al. 2012) that offsets the Main Central Thrust (MCT) and the South Tibet Detachment System (STDS) (Fig. 2.2b). On the eastern side of the Tuting-Basar fault, the MCT and STDS swerve around the Siang window and follow a NW–SE trend. The Siang window is a domal structure defined by a closed trace of the Main Boundary Thrust (MBT) that exposes rocks structurally below the Lesser Himalayan sequence (Acharyya and Saha 2008). Southeast of the Siang window, the MBT is known as the Mishmi thrust that also trends NW–SE. The Trans-Himalayan Lohit batholith, equivalent to the Gangdese batholith of Tibet, is thrust southwestward over a narrow strip of carbonate and argillaceous Tethyan sediments along the NW–SE trending Lohit thrust. Thus all the major faults, e.g. MBT, MCT, STDS and Lohit thrust, are parallel and trend NW–SE in this region. At the intersection of the Aniqiao fault and Lohit thrust, the Yarlung-Tsangpo suture sharply changes direction and becomes roughly parallel to the Lohit thrust (Fig. 2.2b).

The continuation of the Yarlung-Tsangpo suture follows an arcuate path convex to the east until it encounters the Sagaing fault, a major N–S dextral strike slip fault in Myanmar that separates the Burma microplate to the west from the Shan plateau of Asia (Sundaland) to the east (Fig. 2.2a). The northern end of the Sagaing fault splays into several branches, one of which may be continuous with the Mishmi thrust (Vigny et al. 2003). High-grade kyanite and garnet-bearing schists occur in the Katha-Gangaw and Kumon belts parallel to and on the concave side of the suture near the intersection of the Sagaing fault (Fig. 2.2b). An eclogite boulder probably originating from the Kumon range yielded P–T conditions of 12–13 kb and 530–615 °C (Enami et al. 2012). Similar P–T conditions of >14 kb and 550–600 °C were also determined from the high pressure rocks of the Jade Mines belt at the northwestern branch of the Sagiang fault (Goffé et al. 2000). U–Pb zircon dates of 146.5 ± 3.4 Ma (Shi et al. 2008) and 158 ± 2 Ma (Qiu et al. 2009) in jadeitites from the Jade Mines belt indicate subduction in Late Jurassic perhaps beneath the Sundaland margin (Searle and Morley 2011).

2.3.1 Tuting Metavolcanics

The Tuting metavolcanics are structurally continuous with the Jiaresa-Pangxin and Yigongbai ophiolitic sheets at the eastern margin of the Namche Barwa massif (Quanru et al. 2006; Saha et al. 2012). They occur at the intersection of the Lohit thrust and the Anaqiao fault. They are folded, sheared and banded, and are composed of fine-grained greenschist facies rocks with an albite + epidote + chlorite +

sericite ± titanite ± magnetite assemblage (Saha et al. 2012). The primary mineralogy and texture are obliterated, and the porphyroblasts are composed of albite enclosing chlorite, epidote and sericite. Slender actinolite is embedded in chlorite. Late stage quartz-calcite veins are common. Plagiogranite intrusives occur locally within the metavolcanics. The Lohit granodiorite intrudes the Tuting metavolcanics and contains xenoliths of mafic rocks. Geochemistry of the Tuting metavolcanics is consistent with an origin in a supra-subduction zone environment (Saha et al. 2012).

2.3.2 Tidding Serpentinite

In the Dibang and Lohit valleys of northeastern Arunachal Pradesh and southeast of Tuting, the Tethyan sequence is replaced by the Tidding formation comprising imbricate thrust sheets of ophiolitic affinity (Acharyya 1986). The Tuting-Tidding shear zone shows strike-slip movement along the NW–SE direction and represents the Indus Suture Zone in this region (Valdiya, 2010). Extending further southeast into western Myanmar, the Tuting-Tidding shear zone is offset by the transcurrent, right-lateral, strike-slip Sagaing fault. The Myanmar block has moved 300–500 km northward with respect to Southeast Asia along the Sagaing fault (Swe 1972; Hla Maung 1987).

The Tidding formation consists of folded garnetiferous metavolcanics, actinolite-tremolite schist, chlorite schist and marble with slivers of graphite-garnet schist, epidote and leucogranite intrusives (Misra 2009; Singh and Singh 2011). A tabular body of serpentinised peridotite with relict olivine and Cr-spinel occurs in the upper part of the formation. Compositions of Cr-spinels suggest that the serpentinised peridotite is possibly a residue of a depleted mantle source that underwent a high degree of partial melting in a marginal ocean basin (Singh and Singh 2011).

2.3.3 Mayodia Ophiolite

A probable klippen of ophiolitic rocks occurs above the High Himalayan Crystallines at Mayodia, Dibang Valley, northwest of Tidding (Ghosh and Ray 2003; Ghosh et al. 2007). These rocks may be correlated with the Tidding ophiolitic rocks. The Mayodia ophiolitic sequence comprises two units. The lower unit consists of foliated and deformed serpentinised peridotite (wehrlite with $Fo_{89–92}$ olivine) tectonite intruded by hornblendite dikes and overlain by banded amphibolite. The upper unit consists of metabasalt interlayered with metapelite. The metabasalt is folded and comprises actinolite-chlorite-albite-epidote schist indicating greenschist facies metamorphism. The chemical composition of the metabasalt shows similarities with MORB (Ghosh et al. 2007).

2.3.4 Indo-Myanmar Range

The Sagaing fault offsets the continuation of the Yarlung-Tsangpo suture such that the latter is displaced northward on the western side of the fault (Fig. 2.2). Further south, the suture enters the Indo-Myanmar Range (IMR) that consists of predominantly Paleogene flyschoid sediments with Triassic (Carnian) feldspathic turbidites, ophiolite and Triassic-Cretaceous metamorphic rocks including a 30-km-wide mica schist belt (Brunnschweiler 1966; Bender 1983; Mitchell 1993). The suture here represents collision between the Indian plate and the Burma microplate, a westward convex, 1,300 km long plate including continental crust and is demarcated by an ophiolite belt traceable through Nagaland and Manipur including the Naga Hills, the Chin Hills (Mt. Victoria), the Arakan Hills and the Arakan coast of western Myanmar. The Naga/Disang thrust is equivalent to the Main Boundary Thrust (MBT) of the Himalayas and marks the western border of the Paleogene Indo-Myanmar Range. A closely spaced thrust fault to the Disang thrust known as the Tipu thrust is *en echelon* with the Kaladan fault that continues southward and connects with the arcuate Andaman–Sumatra–Java subduction zone (Yin et al. 2010). The India-Burma plate boundary has jumped westward several times during the Cenozoic, and the Kaladan fault marks the present-day plate boundary (Maurin and Rangin 2009). At present, the Indian plate is obliquely subducting beneath the Burma-microplate at the Andaman subduction zone with a velocity of $\sim$4 cm.a^{-1} toward N20°E (Paul et al. 2001; Vigny et al. 2005). The geology of IMR is discussed in detail in Chap. 5.

2.3.5 Andaman Ophiolite

The 850-km-long chain of islands between the Bay of Bengal and the Andaman Sea constitute the Andaman Island Arc. It comprises two nearly parallel arcuate belts. The Andaman Ophiolite is exposed intermittently on the Andaman-Nicobar Islands, a forearc ridge that constitutes a part of the accretionary complex in the outer part of the Andaman Arc referred to as the western arc (Karunakaran et al. 1964; Bandyopadhyay et al. 1973; Halder 1985; Prasad 1985; Vohra et al. 1989; Bandopadhyay 2005). This belt is the southern extension of Naga Hills and Arakan orogenic belt, which swerves southeastwards and continues through the subduction zone offshore of Sumatra. Currently, active arc volcanoes on Barren Island (Ball 1973; 1888;

Haldar and Luhr 2003; Luhr and Haldar 2006) and Narcondam Island (Pal et al. 2007) are located east of the Andaman Islands along the eastern arc that continues southeastward through the Java–Sumatra volcanic chain, and northward into Myanmar where several extinct volcanoes such as Mt Popa and Mt Taungthonlon (Miocene-Quaternary) are found. A back-arc basin exists further east of the Andaman Arc, where the sea floor is spreading from several ENE–WSW ridge segments offset by several N–S right-lateral strike-slipfaults since c. 4 Ma (Raju et al. 2004; Curray 2005). The N–S strike-slip faults are part of an extensive horsetail structure at the southern end of the Sagaing fault of Myanmar (Maurin and Rangin 2009). A 95 ± 2 Ma age of trondhjemite (Pedersen et al. 2010) and 93.6 ± 1.3 Ma age of plagiogranite (Sarma et al. 2010), late-stage derivatives of the Andaman ophiolitic gabbro, constrain the age of formation of the oceanic lithosphere emplaced in the Andaman Ophiolite. The age of obduction of the ophiolite is constrained by the 83.5–70.6 Ma age of radiolarian chert above the ophiolite (Ling et al.1996). On the basis of similarity in age of the 95 ± 2 Ma Andaman Ophiolite, 93.5–97.9 Ma Samail Ophiolite in Oman (Tilton et al. 1981; Warren et al. 2005) and 91.6 ± 1.4 Ma Troodos Ophiolite in Cyprus (Mukasa and Ludden 1987), Pedersen et al. (2010) concluded that these ophiolites formed simultaneously in the fore-arcs of several coexisting trans-Tethyan subduction zones.

The Andaman Ophiolite Group comprises subhorizontal thrust slices that form the basement on which Tertiary accretionary prism sediments were deposited (Sengupta et al. 1990). The ophiolite group is overlain by the Mithakhari Group containing polymictic conglomerate, sandstone, arkose, shale, foraminiferal limestone and pyroclasts in the upper part (Bandopadhyay 2011).

The volcanic rocks of the Andaman Ophiolite belong to the tholeiitic series. Trace element and REE content of the hyaloclastites and pillow basalts are similar to MORB and indicate a back-arc environment (Jafri et al. 2010). Chromite compositions, oxygen fugacity values and trace element compositions of the mantle peridotite units indicate formation of the ophiolite at a mid-oceanic ridge or a supra-subduction zone spreading centre (Pal 2011). However, the upper crust in the southern part also contains andesite and dacite, which suggests that arc-related crust is built on top of the MORB-type oceanic crust (Pedersen et al. 2010). The mantle tectonites are serpentinised and crudely foliated. The orthopyroxene porphyroclasts ($En_{87–88}$) with olivine ($Fo_{89–94}$) and chromite inclusions are resorbed and surrounded by olivine neoblasts (Pal 2011). Large diopsidic clinopyroxene grains are embayed and surrounded by orthopyroxene. The Cr# (100 Cr/(Cr + Al)) of chromite ranges from 20–39 in peridotite to 73–80 in chromitite pods (Ghosh et al. 2009). The composition of the chromites is consistent with their origin in peridotite in a supra-subduction zone. The chromitite pods also contain chromian andradite garnet with up to 50 mol % uvarovite (Ghosh and Morishita 2011). The layered ultramafic–mafic cumulates contain sieve-textured olivine and resorbed chromite. Unaltered olivine ($Fo_{93–90}$) and euhedral chromite are also present in some samples (Pal 2011). Lherzolite cumulates contain resorbed orthopyroxene. Less altered diopside-augite clinopyroxene contains olivine, orthopyroxene and chromite (Cr# 71–73) inclusions. Cumulate gabbro contains olivine ($Fo_{87–78}$) and orthopyroxene (En_{78}) in some samples. P–T estimates based on clinopyroxene thermobarometry yield a wide range of temperatures (500–1000 °C) at 7–8.6 kb pressure for the cumulate pyroxenite and gabbros (Saha et al. 2010).

Alteration is common in the cumulate gabbros with plagioclase showing saussuritisation and pyroxene showing uralitisation and chloritisation. Magnetite-ulvospinel occurs as an accessory phase. Clinopyroxene is altered to amphibole and plagioclase is saussuritised also in the intrusive gabbro and dolerite. The intrusive gabbro grades into quartz-bearing plagiogranite with An_{93} plagioclase, minor hornblende altered to chlorite and accessory magnetite and ilmenite. The basaltic volcanics contain phenocrysts of augite and olivine near the base, and augite and plagioclase near the top. The groundmass is subophitic, intersertal or vitrophyric and consists of albite, epidote, chlorite, altered glass and magnetite. The groundmass of the upper lavas contains glass droplets and intricate veins of carbonate and silica and zeolite. The red charts consist of microcrystalline quartz, clay and iron oxides. The pelagic sedimentary units consist of micritic foraminiferal limestone and carbonate-bearing red clay.

2.4 Summary of Petrographic Features

2.4.1 Waziristan

Ultramafic rocks:

- Dunite layers and lenses in harzburgite contain strained olivine.
- Harzburgite contains olivine (Fo_{91}),orthopyroxene (En_{91}, $Al_2O_3$1.6 wt %) and minor plagioclase.
- Pyroxenite dikes are composed of orthopyroxene ± diopside ± olivine.
- Anorthosite contains zoned plagioclase ($An_{77–73}$) with higher K_2O in the core, and minor clinopyroxene (Mg# 56).
- Podiform chromitite commonly contains zoned alumino-chromite (Cr_2O_3 49–61 wt %) with ferri-chromite rim, and minor amounts of chlorite, serpentine and magnetite (Jan et al. 1985).

2.4.2 Sapat

Meta-harzburgite and dunite with fine-grained, massive texture:

- Relict orthopyroxene and lobate olivine with euhedral spinel inclusions, sub-grain boundaries and undulose extinction; matrix has fine-grained, undeformed olivine neoblasts, disseminated amoeboid spinel and orthopyroxene break down products like olivine, talc and tremolite: fluid-assisted lower amphibolite facies re-equilibration (Bouilhol et al. 2009).
- Trails/pods of chromite spinel and clinopyroxene in dunite, micro-veins and thin dikes of olivine-clinopyroxene: originated through melt percolation.
- Secondary chlorite around spinel, serpentine and rare diopside around olivine and calcite vein in dunite: late stage alteration.

Meta-gabbro and tonalite–trondhjemite with clinopyroxenite intrusives:

- Clinopyroxene overgrows olivine in clinopyroxenite, amoeboid clinopyroxene at grain boundaries of olivine porphyroblasts; trails of lobate clinopyroxene porphyroblasts; secondary chlorite and hornblende: melt-rock interactions.

2.4.3 Spontang

Peridotite with porphyroclastic texture:

- Olivine and orthopyroxene have lobate margins: evidence of mantle melting.
- Exsolution lamellae of diopside-augite in orthopyroxene, and of orthopyroxene in clinopyroxene: sub-solidus equilibration.
- Undulatory extinction and kinks in olivine: deformation during ascent of mantle below spreading center at 1000–1200 °C and low deviatoric stress (Reuber 1986).

Diorite dikes and sills with ophitic to cumulate texture cross-cutting mantle peridotite:

- Hornblende/edenite and albite, minor epidote, oxides, titanite and apatite; hornblende is locally replaced by actinolite: amphibolite to greenschist facies metamorphism.
- Anorthite-rich plagioclase core and diopside inclusions in hornbende/edenite: magmatic relics.

Upper crustal gabbro:

- Plagioclase laths, though commonly altered, are well-preserved: probably crystallised before clinopyroxene in a normal mid-oceanic ridge environment (Corfield et al. 2001).

2.4.4 Nidar

Crustal micro-gabbro with ophitic texture and cumulate gabbro:

- Plagioclase contains olivine inclusions, clinopyroxene contains olivine and plagioclase inclusions and pargasitic hornblende rims clinopyroxene: olivine—plagioclase—clinopyroxene MORB-type crystallisation sequence.
- Large lobate olivine grains and interstitial neoblasts of euhedral olivine and some clinopyroxene: evidence of magmatic reactions.
- An-rich plagioclase core with kink and bent cleavage is rimmed by undeformed plagioclase; lower-Ca clinopyroxene is rimmed by higher-Ca undeformed clinopyroxene, pargasite rim around diopside: deformation followed by amphibolite facies metamorphism.
- Actinolitic amphibole in veins: late stage alteration.

Crustal basalts:

- Phenocrysts of albitic plagioclase laths, diopside-augite, serpentinised olivine, minor Fe–Ti oxides: hydrothermal alteration.
- Groundmass of augite, plagioclase, rare glass, epidote with radiating crystals of chlorite, banded rhyolite with glass and palagonite, feldspar spherules, fibrous chlorite, veins/vesicles with quartz and calcite: hydrothermal alteration.

2.4.5 Yungbwa

Harzburgite with porphyroclastic texture:

- Elongated olivine with kink-bands, orthopyroxene with exsolution lamellae and deformed cleavage showing undulatory extinction and sub-parallel to foliation: mantle deformation.
- Large spinel grains have "holly-leaf" shape.
- Pyroxene inclusions in plagioclase.
- Euhedral neoblasts of olivine, orthopyroxene and clinopyroxene, rounded spinel and disseminated sulphides.
- Minor anorthitic plagioclase and pargasitic amphibole: metasomatic alteration mantle.

Basalt and gabbronorite dikes with sub-ophitic orhypidiomorphic-granular texture:

- Sericitisation of plagioclase and replacement of clinopyroxene and hornblende byactinolite: low-grade metamorphism.
- Recrystallisation and granulation, plagioclase with undulatoryextinction and partial transformation to prehnite-bearing saussurite, clinopyroxene partially replaced by metamorphic hornblende, tremolite or actinolite with a typical flaser texture: low-grade metamorphism.

2.4.6 Xiugugabu

Harzburgite with porphyroclastic to porphyromylonitic texture:
- Kinked and highly stretched olivine and orthopyroxene porphyroclasts with undulatory extinction: mantle deformation.
- Orthopyroxene containing clinopyroxene lamellae surrounded by neoblasts: recrystallisation.
- Minor large euhedral spinel and small vermicular intergrowths, and accessory magnetite, chlorite and amphibole: probably alteration.

Microgabbro and microgabbronoritesills intruding harzburgite:
- Plagioclase crystallised before pyroxene: MORB-type crystallisation sequence.
- Foliation defined by parallel orientation of plagioclase and pyroxene microphenocrysts; magnetite + clinopyroxene symplectite, amphibole + clinopyroxene symplectite and amphibole overgrowth around clinopyroxene: amphibolite facies hydrothermal metamorphism.
- Epidote, chlorite and sericite: secondary alteration.

2.4.7 Zhongba

Harzburgite with minor dunite:
- Fresh and foliated.

Diabase dike with granular- to medium-grained intersertal texture:
- Idiomorphic plagioclase, chloritised pyroxene and olivine and minor Fe–Ti oxides. Texture showing clinopyroxene cores with radiating plagioclase laths is present in some samples.

Porphyritic pillow and massive olivine basalts with intersertal to intergranular texture:
- Phenocrysts are partially replaced by albite or chlorite.
- Secondary veins and amygdules of carbonate, quartz and chlorite.

2.4.8 Saga and Sangsang

Lherzolite and harzburgite:
- Serpentinised near faults or shear zones.
- Large olivine and pyroxene grains show minor folds or kinks and undulatory extinction: mantle deformation.
- Olivine inclusions in pyroxene, minor euhedral spinel.
- Recrystallised, interstitial olivine around clinopyroxene, olivine + clinopyroxene symplectite around orthopyroxene, orthopyroxene + spinel symplectite and vermicular spinel: melt-rock interactions.
- Minor chlorite, actinolite, carbonate and prehnite: secondary alteration and metasomatism.

Gabbro:
- Plagioclase altered to albite + prehnite, clinopyroxene replaced by metamorphic green amphibole or minor chlorite: low-temperature metamorphism.

Mafic to intermediate lava:
- Clinopyroxene altered to actinolite and chlorite, plagioclase microlites and glomerocrysts with pyroxene inclusions altered to albite, prehnite and/or sericite: low-temperature alteration.
- Amygdules filled with chlorite, quartz and carbonate, veins of carbonate and chlorite: secondary alteration.
- Uppermost part brecciated.

Diabase:
- Minor secondary actinolite needles and epidote.

Amphibolite:
- Cloudy plagioclase, metamorphic green hornblende and minor oxides and titanite are highly altered to albite-prehnite-epidote-chlorite assemblages.

Sandstone:
- Clasts of deformed quartz, feldspar, pseudomorphs of pyroxene and hornblende with actinolite and chlorite, spinel, felsic plutonics, mafic to intermediate volcanics, rare radiolarian chert and carbonate oolite and minor chlorite and carbonate: low temperature alteration.

2.4.9 Xigaze

Foliated and serpentinised, spinel and clinopyroxene bearing dunite, harzburgite and lherzolite:
- Porphyroclastic orthopyroxene with clinopyroxene lamellae surrounded by granoblastic olivine showing slip planes and kink bands, or granular orthopyroxene and olivine with interstitial Cr-diopside: mantle deformation.

Pillow basalt with intersertal texture:
- Altered and contains vesicles with quartz, calcite, chlorite and/orepidote.

Diabase:
- Rare hornblende phenocrysts: hydrous magma.
- Subordinate glass and opaques in the groundmass, secondary actinolite and clay minerals.

2.4.10 Luobusa

Diopsidic harzburgite with porphyroclastic texture:
- Rare olivine porphyroclasts with orthopyroxene inclusions show deformation lamellae and kink bands: mantle deformation.

- Fine-grained olivine neoblasts in the granoblastic matrix surrounding subhedral to anhedral orthopyroxene porphyroclasts with clinopyroxene lamellae: olivine replaces orthopyroxene.
- Accessory chromite occurs as euhedral inclusions in olivine and anhedral, ubiquitous grains in the matrix.

2.4.11 Andaman

Foliated, serpentinised mantle tectonite:

- Resorbed orthopyroxene porphyroclasts with olivine and chromite inclusions surrounded by olivine neoblasts; embayed diopside grains surrounded by orthopyroxene: mantle melting reactions.

  Layered ultramafic–mafic cumulates:
- Sieve-textured olivine and resorbed chromite; some unaltered olivine and euhedral chromite.
- Lherzolite cumulates contain resorbed orthopyroxene. less altered diopside-augite with olivine, orthopyroxene and chromite inclusions.
- Cumulate gabbro contains olivine and orthopyroxene in some samples, saussuritised plagioclase and uralitised and chloritised pyroxene and accessory magnetite-ulvospinel.

  Intrusive gabbro and dolerite:
- Clinopyroxene altered to amphibole and plagioclase is saussuritised, minor hornblende altered to chlorite and accessory magnetite andilmenite.

  Basaltic volcanics with subophitic, intersertal or vitrophyric groundmass:
- Phenocrysts of augite and olivine near the base, and augite and plagioclase near the top.
- Groundmass consists of albite, epidote, chlorite, altered glass and magnetite, with glass droplets and intricate veins of carbonate and silica and zeolite in the upper lavas.

  Sediments:
- Chert contains microcrystalline quartz, clay and iron oxides.
- The pelagic sediments consist of micritic foraminiferal limestone and carbonate-bearing red clay.

References

Acharyya SK, (1986) Cenozoic plate motions creating the EasternHimalaya and Indo-Burmese range around the northeast corner ofIndia. In:Ghose, N.C.and Varadarajan, S., (eds.), "Ophiolites and Indian Plate Margins", Patna University, Patna, 143–160

Acharyya SK, Saha P (2008) Geological setting of the Siang Dome located at the Eastern Himalayan Syntaxis. Extended abstracts: 23rd Himalayan-Karakoram-Tibet workshop, India. Himal J Sci 5:16–17

Ahmad T, Tanaka T, Sachan HK, Asahara Y, Islam R, Khanna PP (2008) Geochemical and isotopic constraints on the age and origin of the Nidar Ophiolitic Complex, Ladakh, India: implications for the Neo-Tethyan subduction along the Indus suture zone. Tectonophysics 451:206–224

Ahmad Z, Abbas SG (1979) The Muslim Bagh ophiolites. In: Farah A, Delong KA (eds) Geodynamics of Pakistan. Geological Survey of Pakistan, Quetta, 243–249

Ahmed Z (1993) Leucocratic rocks from the Bela ophiolite, Khuzadrdistrict, Pakistan. In: Searle MP, Treloar PJ (eds.) Himalayan Tectonics. Geological Society of London Special Publication 74, pp 89–100

Aitchison JC, Davis AM (2004) Evidence for the multiphase nature of the India–Asia collision from the Yarlung Tsangpo suture zone, Tibet. In: Malpas JG, Fletcher CJN, Ali JR, Aitchison JC (eds) Aspects of the tectonic evolution of China. Geological Society of London Special Publication 226: 217–233

Aitchison JC, Davis AM, Abrajevitch AV, Ali JR, Badengzhu Liu J, Luo H, McDermid IRC, Ziabrev SV (2003) Stratigraphic and sedimentological constraints on the age and tectonic evolution of the Neotethyan ophiolites along the Yarlung Tsangpo suture zone, Tibet. In: Dilek Y, Robinson PT (eds) Ophiolites in earth history. Geological Society, London, Special Publications, 218: 147–164

Allègre CJ, Courtillot V, Tapponnier P, Hirn A, Mattauer M, Coulon C et al (1984) Structure and evolution of the Himalaya–Tibet orogenic belt. Nature 307:17–22

Alleman F (1979) Time of emplacement of the Zhob valley ophiolites and Bela ophiolites, Balochistan (preliminary report). In: Farah A, DeJong KA (eds) Geodynamics of Pakistan. Geological Survey of Pakistan, Quetta, 215–242

Arif M, Jan Q (2006) Petrogenetic significance of the chemistry of chromite in the ultramafic–mafic complexes. J Asian Earth Sci 27:628–646

Asrarullah AZ, Abbas SG (1979) Ophiolites in Pakistan: introduction. In: Farah A, Dejong KA (eds) Geodynamics of Pakistan. Geological Survey of Pakistan, Quetta, 181–192

Ball V (1888) The volcanoes of Barren Island and Narcondam in the Bay of Bengal. Geol Mag 9:404–408

Bandopadhyay PC (2005) Discovery of abundant pyroclasts in the Namunagarh grit, South Andaman: evidence for arc volcanism and active subduction during the Palaeogene in the Andaman area. J Asian Earth Sci 25:95–107

Bandopadhyay PC (2011) Re-interpretation of the age and environment of deposition of paleogene turbidites in the Andaman and Nicobar Islands, Western Sunda Arc. J Asian Earth Sci. doi: 10.1016/j.jseaes.2011.08.018

Bandyopadhyay S, Subramanyam MR, Sharma PN (1973) The geology and mineral resources of the Andaman and Nicobar Islands. Rec Geol Surv India 105:25–68

Baxter AT, Aitchison JC, Ali JR, Zyabrev SV (2010) Early Cretaceous radiolarians from the Spongtang massif, Ladakh, NW India: implications for Neo-Tethyan evolution. J Geol Soc Lond 167:511–517

Bédard É, Hébert R, Guilmette C, Lesage G, Wang CS, Dostal J (2009) Petrology and geochemistry of the Saga and Sangsang ophiolitic massifs, Yarlung-Zangbo Suture Zone, Southern Tibet: evidence for an arc–back-arc origin. Lithos 113:48–67

Bender F (1983) Geology of Burma. Gebruder Borntraeger, Berlin 293p

Berthelsen A (1953) On the geology of the Rupshu District, N.W. Himalaya: Meddelelser fra Dansk Geologisk Forening 12:350–415

Bezard R, Hébert R, Wang C, Dostal J, Dai J, Zhong H (2011) Petrology and geochemistry of the Xiugugabu ophiolitic massif, western Yarlung Zangbo suture zone, Tibet. Lithos 125:347–367

Bhattacharjee CG (1991) The ophiolites of northeast India—a subduction zone ophiolite complex of the Indo-Burman orogenic belt. Tectonophysics 191:213–222

Bouilhol P, Burg JP, Bodinier JL, Scmidt MW, Dawood H, Hussain S (2009) Magma and fluid percolation in arc to forearc mantle: evidence from Sapat (Kohistan, Northern Pakistan). Lithos 107:17–37

Brunnschweiler RO (1966) On the geology of the Indoburman ranges. J Geol Soc Aust 11:117–194

Burg JP, Nievergelt P, Oberli F, Seward D, Davy P, Maurin JC, Diao ZZ, Meier M (1998) The Namche Barwa syntaxis: evidence for exhumation related to compressional crustal folding. J Asian Earth Sci 16:239–252

Chan GH-N, Crowley Q, Searle M, Aitchison JC, Horstwood M (2007) U–Pb zircon ages of the Yarlung Zangbo suture zone ophiolites, south Tibet. In: 22th Himalaya–Karakoram–Tibet workshop, Hong Kong, China, workshop abstract, vol 12

Constantin M (1999) Gabbroic intrusions and magmatic metasomatismin harzburgites from the Garrett transform fault: implications for the nature of the mantle—crust transition at fast spreading ridges. Contrib Miner Petrol 136:111–130

Corfield RI, Searle MP, Pedersen RB (2001) Tectonic setting and obduction history of the Spontang ophiolite, Ladakh Himalaya, NW India. J Geol 109:715–736

Corfield RI, Watts AB, Searle MP (2005) Subsidence of the North Indian Continental Margin, Zanskar Himalaya, NW India. J Geol Soc Lond 162:135–146

Curray JR (2005) Tectonics and history of the Andaman Sea region. J Asian Earth Sci 25:187–232

Dai J-G, Wang C-S, Hébert R, Santosh M, Li Y-L, Xu J-Y (2011) Petrology and geochemistry of peridotites in the Zhongba ophiolite, Yarlung Zangbo Suture Zone: Implications for the Early Cretaceous intra-oceanic subduction zone within the Neo-Tethys. Chem Geol 288:133–148

Dai J, Wang C, Li Y (2012) Relicts of the Early Cretaceous seamounts in the central-western Yarlung Zangbo Suture Zone, southern Tibet. J Asian Earth Sci 53:25–37

de Sigoyer J, Guillot S, Dick P (2004) Exhumation of the ultrahigh-pressure Tso Morari unit in eastern Ladakh (NW Himalaya): a case study: Tectonics 23:TC3003

Dietrich VJ, Frank W, Honegger K (1983) A Jurassic–Cretaceousisland arc in the Ladakh–Himalaya. J Volcanol Geoth Res 18:405–433

Ding L, Zhong DL, Yin A, Kapp P, Harrison TM (2001) Cenozoic structural and metamorphic evolutionof the eastern Himalayan syntaxis (Namche Barwa). Earth Planet Sci Lett 192:423–438

Dubois-Côté V, Hébert R, Dupuis C, Wang CS, Li YL, Dostal J (2005) Petrological and geochemical evidence for the origin of the Yarlung Zangbo ophiolites, southern Tibet. Chem Geol 214:265–286

Dupuis C, Hébert R, Dubois-Côté V, Wang CS, Li YL, Li ZJ (2005) Petrology and geochemistry of mafic rocks from mélange and flysch units adjacent to the Yarlung Zangbo Suture Zone, southern Tibet. Chem Geol 214:287–308

Enami M, Ko ZW, Win A, Tsuboi M (2012) Eclogite from the Kumon range, Myanmar: petrology and tectonic implications. Gondwana Res 21:548–558

Gansser A (1964) Geology of the Himalayas. Wiley Interscience, London 289 p

Gansser A (1980) The significance of the Himalayan suture zone. Tectonophysics 62:37–52

Garzanti E, Sciunnach D, Gaetani M, Corfield RI, Watts AB, Searle MP (2005) Discussion on subsidence history of the north Indian continental margin, Zanskar–Ladakh Himalaya, NW India. J Geol Soc Lond 162:889–892

Ghosh B, Morishita T (2011) Andradite-uvarovite solid solution from hydrothermally altered podiform chromitite, Rutland ophiolite, Andaman, India. Can Mineral 49:573–580

Ghosh B, Ray J (2003) Mineral chemistry of ophiolitic rocks of Mayodia–Hunli area of Dibang valley district, Arunachal Pradesh, Northeastern India. Mem Geol Soc India 52:447–471

Ghosh B, Mahoney J, Ray J (2007) Mayodia Ophiolites of Arunachal Pradesh, Northeastern Himalaya. J Geol Soc India 70:595–604

Ghosh B, Pal T, Bhattacharya A, Das D (2009) Petrogenetic implications of ophiolitic chromite from Rutland Island, Andaman—a boninitic parentage in suprasubduction setting. Mineral Petrol 96:59–70

Girardeau J, Mercier J-CC (1988) Petrology and texture of the ultramafic rocks of the Xigaze ophiolite (Tibet): constraints for mantle structure beneath slow-spreading ridges. Tectonophysics 147:33–58

Girardeau J, Mercier J-CC, Xibin W (1985a) Petrology of the mafic rocks of the Xigaze ophiolite, Tibet: implications for the genesis of the oceanic lithosphere. Contribrib Mineral Petrol 90:309–321

Girardeau J, Mercier J-CC, Yougong Z (1985b) Origin of the Xigaze ophiolite, Yarlung Zangbo suture zone, southern Tibet. Tectonophysics 119:407–433

Gnos E, Immenhauser A, Peter T (1997) Late Cretaceous/early Tertiary convergence between the Indian and Arabian plates recorded in ophiolites and related sediments. Tectonophysics 271:1–19

Gnos E, Khan M, Mahmood K, Villa IM, Khan AS (1998) Bela oceanic lithosphere assemblage and its relation to the Réunion hotspot. Terra Nova 10:90–95

Göpel C, Allègre CJ, Xu R-H (1984) Lead isotopic study of the Xigaze ophiolite (Tibet): the problem of the relationship between magmatites (gabbros, dolerites, lavas) and tectonites (harzburgites). Earth Planet Sci Lett 69:301–310

Guilmette C, Hébert R, Dupuis C, Wang CS, Li ZJ (2008) Metamorphic history and geodynamic significance of high-grade metabasites from the ophiolitic melange beneath the Yarlung Zangbo ophiolites, Xigaze area, Tibet. J Asian Earth Sci 32:423–437

Guilmette C, Hébert R, Wang C, Villeneuve M (2009) Geochemistry and geochronology of the metamorphic sole underlying the Xigaze Ophiolite, Yarlung Zangbo Suture Zone, South Tibet. Lithos 112:149–162

Guilmette C, Hébert R, Dostal J, Indares A, Ullrich T, Bédard E, Wang C (2012) Discovery of a dismembered metamorphic sole in the Saga ophiolitic mélange, South Tibet: assessing an Early Cretaceous disruption of the Neo-Tethyan supra-subduction zone and consequences on basin closing. Gondwana Res 22(2):398–414

Halder D (1985) Some aspect of the Andaman ophiolite complex. Geol Surv India 115Pt(2):1–11

Halder D, Luhr JF (2003) The Barren Island volcanism during 1991 and 1994–95: Eruption style and lava petrology. Mem Geol Surv India 52:313–338

Hébert R, Bezard R, Guilmette C, Dostal J, Wang CS, Liu ZF (2012) The Indus–Yarlung Zangbo ophiolites from Nanga Parbat to Namche Barwa syntaxes, southern Tibet: First synthesis of petrology, geochemistry, and geochronology with incidences on geodynamic reconstructions of Neo-Tethys. Gondwana Res 22(2):377–397

Hodges KV (2000) Tectonics of the Himalaya and southern Tibet from two perspectives. Geol Soc Am Bull 112:324–350

Honegger K, Dietrich V, Frank W, Gansser A, Thoni M, Trommsdorf V (1982) Magmatic and metamorphism in the Ladakh Himalayas (the Indus–Tsangpo suturezone). Earth Planet Sci Lett 60:253–292

Honegger K, Le Fort P, Mascle G, Zimmermann JL (1989) The blueschists along the Indus Suture Zone in Ladakh, NW Himalaya. J Metamorph Geol 7:57–72

Jafri SH, Sarma DS, Sheikh JM (2010) Hyaloclastites in pillow basalts, South Andaman Island, Bay of Bengal, India. Curr Sci 99(12):1825–1829

Jan MQ, Windley BF, Khan A (1985) The Waziristan ophiolite, Pakistan: general geology and chemistry of chromite and associated phases. Econ Geol 80:294–306

Karunakaran C, Pawde MB, Raina VK, Ray KK (1964) Proceeding 22nd International Geological Congress, New Delhi, vol 11, 79–100

Li JF, Xia B, Liu LW, Xu LF, He GS, Wang H, Zhang YQ, Yang ZQ (2009) SHRIMP U–Pb dating for the gabbro in Qunrang Ophiolite, Tibet: the geochronology constraint for the development of eastern Tethys basin. Geotectonica et Metallogenia 33:294–298

Ling HY, Chandra R, Karkare SG (1996) Tectonic significance of Eocene and Cretaceous radiolaria from South Andaman Island, northeast Indian Ocean. Island Arc 5:166–179

Liu C-Z, Wu F-Y, Wilde SA, Yu L-J, Li JL (2010) Anorthitic plagioclase and pargasitic amphibole in mantle peridotites from the Yungbwa ophiolite (southwestern Tibetan Plateau) formed by hydrous melt metasomatism. Lithos 114:413–422

Luhr JF, Haldar D (2006) Barren Island Volcano (NE Indian Ocean): Island arc high-alumina basalts produced by troctolite contamination. J Volcanol Geotherm Res 149:177–212

Mahéo G, Bertrand H, Guillot S, Villa IM, Keller F, Capiez P (2004) The South Ladakh ophiolites (NW Himalaya, India): an intra-oceanic tholeiitic arc origin with implication for the closure of the Neo-Tethys. Chem Geol 203:273–303

Mahmood K, Boudier F, Gnos E, Monie P, Nicolas A (1995) 40Ar/39Ar dating of the emplacement of the Muslim Bagh ophiolite, Pakistan. Tectonophysics 250:169–181

Malpas J, Zhou MF, Robinson PT, Reynolds PH (2003) Geochemical and geochronological constraints on the origin and emplacement of the Yarlung Zangbo ophiolites, Southern Tibet. In: Dilek Y, Robinson PT (eds) Ophiolites in earth history. Geological Society of London Special Publication 218, pp 191–206

Maung Hla (1987) Transcurrent movements in the Burma–Andaman Sea region. Geology 15:911–912

Maurin T, Rangin C (2009) Structure and kinematics of the Indo-Burmese Wedge: recent and fast growth of the outer wedge. Tectonics 28:TC2010

McDermid IRC, Aitchison JC, Davis AM, Harrison TM, Grove M (2002) The Zedong Terrane: a Late Jurassic intra-oceanic magmatic arc within the Yarlung Zangbo suture zone, southeastern Tibet. Chem Geol 187:267–277

Miller C, Thöni M, Frank W, Schuster R, Melcher F, Meisel T, Zanetti A (2003) Geochemistry and tectonomagmatic affinity of the Yungbwa ophiolite, SW Tibet. Lithos 66:155–172

Misra DK (2009) Litho-tectonic sequence and their regional correlation along the Lohit and Dibang Valleys, Eastern Arunachal Pradesh. J Geol Soc India 73:213–219

Mitchell AHG (1993) Cretaceous-Cenozoic tectonicevents in the western Myanmar (Burma)-Assam region. J Geol Soc Lond 150:1012–1089

Mitchell AHG, Htay MT, Htun KM, Win MN, Oo T, Hlaing T (2007) Rock relationships in the Mogok metamorphic belt, Tatkon to Mandalay, central Myanmar. J Asian Earth Sci 29:891–910

Mukasa SB, Ludden JN (1987) Uranium–lead isotopic ages of plagiogranites from the Troodos ophiolite, Cyprus, and their tectonic significance. Geology 15:825–828

Nicolas A, Girardeau J, Marcoux J, Dupré B, Wang X, Cao Y, Zheng H, Xiao X (1981) The Xigaze ophiolite (Tibet): a peculiar oceanic lithosphere. Nature 294:414–417

Pal T (2011) Petrology and geochemistry of the Andaman ophiolite: melt–rock interaction in a suprasubduction-zone setting. J Geol Soc Lond 168:1031–1045

Pal T, Mitra SK, Sengupta S, Katari A, Bandopadhyay PC, Bhattacharya AK (2007) Dacite–andesites of Narcondam volcano in the Andaman Sea—an imprint of magma mixing in the inner arc of the Andaman–Java subduction system. J Volcanol Geotherm Res 168:93–113

Paul J, Burgmann R, Gaur VK, Bilham R, Larson KM, Ananda MB, Jade S, Mukal M, Anupama TS, Satyal G, Kumar D (2001) The motion and and active deformation of India. Geophys Res Lett 28:647–650

Pedersen RB, Searle MP, Corfield RI (2001) U–Pb zircon ages from the Spontang Ophiolite, Ladakh Himalaya. J Geol Soc Lond 158:513–520

Pedersen RB, Searle MP, Carter A, Bandopadhyay PC (2010) U–Pb zircon age of the Andaman ophiolite: implications for the beginning of subduction beneath the Andaman–Sumatra arc. J Geol Soc Lond 167:1105–1112

Prasad U (1985) Ophiolites of India. Rec Geol Surv India 115Pt(2):13–24

Qiu Z, Wu F, Yang S, Zhu M, Sun J, Yang P (2009) Age and genesis of the Myanmar jadeite: constraints from U–Pb ages and Hf isotopes of zircon inclusions. Chin Sci Bull 54(4):658–668

Quanru G, Pan GT, Zheng LL, Chen ZL, Fisher RD, Sun ZM, Ou CS, Dong H, Wang XW, Li S, Lou XY, Fu H (2006) The eastern Himalayan syntaxis: major tectonic domains, ophiolitic mélanges and geologic evolution. J Asian Earth Sci 27:265–285

Radhakrishna T, Divakara Rao V, Murali AV (1984) Geochemistry of Dras volcanlcs and the evolution of the Indus suture ophiolites. Tectonophysics 108:135–153

Radhakrishna T, Divakara Rao V, Murali AV (1987) Geochemistry and petrogenesis of ultramafic and mafic plutonic rocks of the Dras ophiolitic melange, Indus suture (northwest Himalaya). Earth Planet Sci Lett 82:136–144

Raju KA, Ramprasad T, Rao PS, Rao R, Varghese J (2004) New insights into the tectonic evolution of the Andaman basin, northeast Indian Ocean. Earth Planet Sci Lett 221:145–162

Rao DR, Rai H, Senthil Kumar J (2004) Origin of oceanic plagiogranite in the Nidar ophiolitic sequence of eastern Ladakh, India. Curr Sci 87(7):999–1005

Reuber I (1986) Geometry of accretion and oceanic thrusting of Spontang ophiolite, Ladakh-Himalaya. Nature 321:592–596

Reuber I, Montigny R, Thuizat R, Heitz A (1989) K-Ar ages of ophiolites and arc volcanics of the Indus suture zone: clues on the early evolution of the Neo-Tethys. Eclogae Geologische Helvetiae 82/2:699–715

Robertson AHF, Degnan PJ (1993) Sedimentology and tectonic implications of the Lamayuru Complex: deep-water facies of the Indian passive margin, Indus Suture Zone, Ladakh Himalaya. Geol Soc Lond Spec Publ 74:299–321

Saha A, Dhang A, Ray J, Chakraborty S, Moecher D (2010) Complete preservation of ophiolite suite from south Andaman, India: a mineral-chemical perspective. J Earth Syst Sci 119/3:1–16

Saha P, Acharyya SK, Balaram V, Roy P (2012) Geochemistry and tectonic setting of Tuting metavolcanic rocks of possible ophiolitic affinity from Eastern Himalayan Syntaxis. J Geol Soc India 80:167–176

Sarma DS, Jafri SH, Fletcher IR, McNaughton NJ (2010) Constraints on the Tectonic Setting of the Andaman Ophiolites, Bay of Bengal, India, from SHRIMP U–Pb Zircon Geochronology of Plagiogranite. J Geol 118:691–697

Schärer U, Hamet J, Allegre J (1984) The trans-Himalaya (Gangdese) plutonism in the Ladakh region:a U–Pb and Rb-Sr study. Earth Planet Sci Lett 67:327–339

Searle MP, Morley CK (2011) Tectonic and thermal evolution of Thailand in the regional context of SE Asia. In: Ridd MF, Barber AJ, Crow MJ (eds) The geology of Thailand. Geological Society, London, 539–571

Searle MP, Cooper DJW, Rex AJ (1988) Collision tectonics of the Ladakh-Zanskar Himalaya. In: Shackleton RM, Dewey JF, Windley BF (eds) Tectonic evolution of the Himalayas and Tibet. The Royal Society, London, 117–149

Sengupta S, Ray KK, Acharyya SK, de Smeth JB (1990) Nature of ophiolite occurrences along the eastern margin of the Indian plate and their tectonic significance. Geology 18:439–442

Sharma KK, Sinha AK, Bagdasarian GP, Gukasian P (1979) Potassium-argon dating of Dras volcanics. Shyok volcanics and Ladakh granite, Ladakh, Northwest Himalaya. In: Nautiyal SP (ed) Himalayan geology. Wadia Institute of Himalayan Geology, vol 8. Hindustan Publishers, New Delhi, pp 288–295

Shi G, Cui W, Cao S, Jiang N, Jian P, Liu D, Miao L, Chu B (2008) Ion microprobe zircon U–Pb age and geochemistry of the Myanmar jadeitite. J Geol Soc Lond 165:221–234

Singh AK, Singh RKB (2011) Zn- and Mn-rich chrome-spinels in serpentinite of Tidding Suture Zone, Eastern Himalaya and their metamorphism and genetic significance. Curr Sci 100(5):743–749

Sinha AK, Upadhyay R (1993) Mesozoic neo-tethyan pre-orogenic deep marine sediments along the Indus–Yarlung Suture, Himalaya. Terra Res 271–281

Srikantia SV (1986) Tectonic design of the Ladakh region, India. In: Ghose NC, Varadarajan S (eds) Ophiolites and Indian plate margin. Sumna Publications, Patna, pp 29–47

Srikantia SV, Razdan ML (1980) Geology of part of central Ladakh Himalaya with particular reference to the Indus Tectonic Zone. J Geol Soc India 21:523–545

Srikantia SV, Razdan ML (1985) The Indus tectonic zone of the Ladakh Himalaya: its geology, tectonics and ophiolite occurrence. Geol Surv India Rec 115:61–92

Swe W (1972) Strike-slip faulting in Central Burma. In: Haile NH (ed) In: Regional conference on geology of Southeast Asia, Geological Society of Malayasia, Kuala Lampur, pp 59–61

Tapponnier P, Mercier JL, Proust F, Andrieux J, Armijo R, Bassoullet JP et al (1981) The Tibetan side of the India–Eurasia collision. Nature 294:405–410

Thakur VC (1981) Regional framework and geodynamic evolution of the Indus–Tsangpo suture zone in the Ladakh Himalayas. Trans R Soc Edinb Earth Sci 72:89–97

Thakur VC, Misra DK (1984) Tectonic framework of Indus and Shyok Suture Zones in eastern Ladakh. Northwest Himalaya. Tectonophysics 101:207–220

Tilton GR, Hopson CA, Wright JE (1981) Uranium–lead isotopic ages of the Semail Ophiolite, Oman, with applications to Tethyan ridge tectonics. J Geophys Res 86:2763–2775

Valdiya KS (1988) Tectonic evolution of the central sector of Himalaya. Philos Trans Royal Soc Lond A326:151–175

Valdiya KS (2010) The making of India : Geodynamic evolution. Macmillan Publishers India Ltd., New Delhi 816 p

Vigny C, Socquet A, Rangin C, Chamot-Rooke N, Pubellier M, Bouin M-N, Bertrand G, Becker M (2003) Present-day crustal deformation around Sagaing fault, Myanmar. J Geophys Res 108/B11:2533

Vigny C, Simons WJF, Abu S et al (2005) Insight into the 2004 Sumatra–Andaman earthquake from GPS measurements in Southeast Asia. Nature 436:201–206

Virdi NS (1987) Northern margin of the Indian plate—some lithotectonic constraints. Tectonophysics 134:29–38

Virdi NS (1989) Glaucophane metamorphism in the ophiolite belt of the Indus–Tsangpo zone in the Himalaya. In: Ghose NC (ed) Phanerozoic ophiolites of India. Sumna Publishers, Patna, pp 73–91

Virdi NS, Thakur VC, Kumar S (1977) Blueschist facies metamorphism from the Indus suture zone of Ladakh and its significance. Himal Geol 7:479–482

Vohra CP, Haldar D, Ghosh Roy AK (1989) The Andaman-Nicobar ophiolite complex and associated mineral resources—current appraisal. In: Ghose NC (ed) Phanerozoic ophiolites of India. Sumna Publishers, Patna, pp 381–315

Wang R, Xia B, Zhou G, Zhang Y, Yang Z, Li W, Wei D, Zhong L, Xu L (2006) SHRIMP zircon U-Pb dating for gabbro from the Tiding ophiolite in Tibet. Chinese Science Bulletin 51:1776–1779

Warren CJ, Parrish RR, Waters DJ, Searle MP (2005) Dating the geologic history of Oman's Semail Ophiolite: insights from U–Pb geochronology. Contrib Miner Petrol 150:403–422

Wei ZQ, Xia B, Zhang YQ, Wang R (2006) SHRIMP zircon dating of diabase in the Xiugugabu ophiolite in Tibet and its geological implications. Geotectonica et Metallogenia 30:93–97

White LT, Lister GS (2012) The collision of India with Asia. J Geodyn 56–57:7–17

Xia B, Li JF, Liu LW, Xu LF, He GS, Wang H, Zhang YQ, Yang ZQ (2008) SHRIMP U–Pb dating for diabase in Sangsang ophiolite, Xizang, China: Geochronological constraint for development of eastern Tethys basin. Geochimica 37:399–403

Yin A, Dubey CS, Kelty TK, Webb AAG, Harrison TM, Chou CY, Célérier J (2010) Geologic correlation of the Himalayan orogen and Indian craton: part 2. structural geology, geochronology, and tectonic evolution of the Eastern Himalaya. Geol Soc Am Bull 122:360–395

Zhong LF, XIa B, Zhang YQ, Wang R, Wei DL, Yang ZQ (2006) SHRIMP age determination of Diabase in Luobusa ophiolite, southern Xizang (Tibet).Geol Rev 52:224–229

Zhou M-F, Robinson PT, Malpas J, Li Z (1996) Podiform chromitites in the Luobusa Ophiolite (Southern Tibet): implications for melt-rock interaction and chromite segregation in the upper mantle. J Petrol 37(1):3–21

Zyabrev SV, Aitchison JC, Badengzhu, Davis AM, Luo H, Malpas J (1999) Radiolarian biostratigraphy of supra-ophiolite sequences in the Xigaze area, Yarlung Tsangpo suture, southern Tibet (preliminary report). Radiolaria 17:13–19

Zyabrev SV, Kojima S, Ahmad T (2008) Radiolarian biostratigraphic constraints on the generation of the Nidar ophiolite and the onset of Dras arc volcanism: Tracing the evolution of the closing Tethys along the Indus–Yarlung-Tsangpo suture. Stratigraphy 5/1:99–112

http://www.springer.com/978-81-322-1568-4

A Petrographic Atlas of Ophiolite
An example from the eastern India-Asia collision zone
Ghose, N.; Chatterjee, N.; Fareeduddin
2014, XVII, 234 p. 477 illus., 410 illus. in color.,
Hardcover
ISBN: 978-81-322-1568-4